NEOPLASIA
www.neoplasia.com

Volume 10 Number 9 September 2008 pp. 987–995 **987**

Host A_{2B} Adenosine Receptors Promote Carcinoma Growth[1]

Sergey Ryzhov[*,§], Sergey V. Novitskiy[†,§], Rinat Zaynagetdinov[*,§], Anna E. Goldstein[‡,¶], David P. Carbone[†,§], Italo Biaggioni[‡,§,¶], Mikhail M. Dikov[†,§] and Igor Feoktistov[*,§,¶]

*Division of Cardiovascular Medicine, Vanderbilt University, Nashville, TN 37232, USA; [†]Division of Hematology/Oncology, Vanderbilt University, Nashville, TN 37232, USA; [‡]Division of Clinical Pharmacology, Vanderbilt University, Nashville, TN 37232, USA; [§]Department of Medicine, Vanderbilt University, Nashville, TN 37232, USA; [¶]Department of Pharmacology, Vanderbilt University, Nashville, TN 37232, USA

Abstract

Recent studies suggest that tumor-infiltrating immune cells can benefit the tumor by producing factors that promote angiogenesis and suppress immunity. Because the tumor microenvironment is characterized by high adenosine levels, we hypothesized that the low-affinity A_{2B} adenosine receptor located on host immune cells may participate in these effects. In the current study, we tested this hypothesis in a Lewis lung carcinoma isograft model using A_{2B} receptor knockout (A_{2B}KO) mice. These mice exhibited significantly attenuated tumor growth and longer survival times after inoculation with Lewis lung carcinoma compared to wild type (WT) controls. Lewis lung carcinoma tumors in A_{2B}KO mice contained significantly lower levels of vascular endothelial growth factor (VEGF) compared to tumors growing in WT animals. This difference was due to VEGF production by host cells, which comprised 30 ± 2% of total tumor cell population. Stimulation of adenosine receptors on WT tumor-infiltrating $CD45^+$ immune cells increased VEGF production fivefold, an effect not seen in tumor-associated $CD45^+$ immune cells lacking A_{2B} receptors. In contrast, we found no significant difference in VEGF production between $CD45^-$ tumor cells isolated from WT and A_{2B}KO mice. Thus, our data suggest that tumor cells promote their growth by exploiting A_{2B} adenosine receptor–dependent regulation of VEGF in host immune cells.

Neoplasia (2008) 10, 987–995

Abbreviations: A_{2B}KO, A_{2B} adenosine receptor knockout; CGS21680, 2-*p*[2-carboxyethyl]phenethylamino-5′-*N*-ethylcarboxamidoadenosine; CVT-6883, 3-ethyl-1-propyl-8-{1-[3-(trifluoromethyl)benzyl]-1*H*-pyrazol-4-yl}-3,7-dihydro-1*H*-purine-2,6-dione; DMSO, dimethyl sulfoxide; FITC, fluorescein isothiocyanate; LLC, Lewis lung carcinoma; NECA, 5′-*N*-ethylcarboxamidoadenosine; RT-PCR, reverse transcription–polymerase chain reaction; SCH58261, 5-amino-7-(phenylethyl)-2-(2-furyl)-pyrazolo-[4,3-*e*]-1,2,4-triazolo-[1,5-*c*]-pyrimidine; VEGF, vascular endothelial growth factor; WT, wild type

Address all correspondence to: Igor Feoktistov, PhD, 360 PRB, Vanderbilt University, 2220 Pierce Ave, Nashville, TN 37232-6300. E-mail: igor.feoktistov@vanderbilt.edu

[1]Portions of this work were supported by the US National Institutes of Health grants R01 HL076306 (I. Feoktistov), R01 CA100562 (M.M. Dikov), and R01 CA76321 (D.P. Carbone), by a research grant from Histiocytosis Association of America (M.M. Dikov), and the by American Heart Association Southeastern Affiliate Grant-in-Aid 0755221B (I. Feoktistov). I. Biaggioni and I. Feoktistov hold a patent relating to A_{2B} antagonists, which has been licensed to CV Therapeutics, Inc. (Palo Alto, CA), and have received research funding from this company.
Received 12 April 2008; Revised 18 June 2008; Accepted 20 June 2008

DOI 10.1593/neo.08478

Introduction

Adenosine is an intermediate product in the metabolism of ATP. The release of adenosine is dependent on the metabolic state of a cell. An increase in energy consumption or a decrease in oxygen supply leads to an enhanced production of adenosine. Metabolically active solid tumors grow rapidly and routinely experience severe hypoxia and necrosis that cause adenine nucleotide degradation and adenosine release. Levels of extracellular adenosine are increased in tumor microenvironments also due to the changes in activities of enzymes involved in adenosine metabolism [1,2]. Predictably, several studies demonstrated an increase in adenosine levels in the tumor interstitium reaching concentrations in the micromolar range [3,4], compared to physiological interstitial levels of 30 to 300 nM found in normal tissues [5].

Adenosine has dual functions as a metabolite and as a regulator of cellular functions. The regulatory functions of adenosine are mediated through cell surface G protein–coupled adenosine receptors. Four subtypes of adenosine receptors have been cloned and classified as A_1, A_{2A}, A_{2B}, and A_3 [5]. Among adenosine receptors, the A_{2B} subtype has the lowest affinity to adenosine. In contrast to other adenosine receptor subtypes, A_{2B} receptors are thought to remain silent under normal physiological conditions when interstitial adenosine levels are low and become active only when adenosine levels rise to micromolar concentrations [6].

A_{2B} receptors are ubiquitously distributed in normal tissues [7]. They have been pharmacologically characterized in several cancer cell lines [8–14]. Analysis of gene expression in primary human tumors uncovered overexpression of A_{2B} adenosine receptors in cancer tissues, suggesting their potential role in cancer biology [15]. We and others have shown previously that stimulation of A_{2B} receptors in cancer cell lines up-regulates the production of angiogenic factors, suggesting that tumor A_{2B} receptors may promote neovascularization [10,16,17]. Virtually all tumors arise within a permissive environment associated with the production of factors that induce angiogenesis and modify immunity [18]. Most tumors have been shown to contain an immune infiltrate, which was long thought to represent the host response to the malignancy. However, recent studies suggest that the immune cells may actually benefit the tumor by producing a protumor microenvironment [19]. It is possible, therefore, that not only adenosine receptors located on cancerous cells but also host A_{2B} adenosine receptors may participate in protecting malignant tissue. In the current study, we tested this hypothesis in a Lewis lung carcinoma (LLC) isograft model using wild type (WT) and A_{2B} adenosine receptor knockout (A_{2B}KO) mice.

Materials and Methods

Reagents

5-Amino-7-(phenylethyl)-2-(2-furyl)-pyrazolo-[4,3-*e*]-1,2,4-triazolo-[1,5-*c*]-pyrimidine (SCH58261) was a gift from Drs. C. Zocchi and E. Ongini (Schering Plough Research Institute, Milan, Italy). 3-Ethyl-1-propyl-8-{1-[3-(trifluoromethyl)benzyl]-1*H*-pyrazol-4-yl}-3,7-dihydro-1*H*-purine-2,6-dione (CVT-6883) was provided by CV Therapeutic, Inc. (Palo Alto, CA) under a sponsored research agreement. Adenosine, 2-*p*[2-carboxyethyl]phenethylamino-5′-*N*-ethylcarboxamidoadenosine (CGS21680), 5′-*N*-ethylcarboxamidoadenosine (NECA), and dimethyl sulfoxide (DMSO) were purchased from Sigma (St. Louis, MO). When used as a solvent, final DMSO concentrations in all assays did not exceed 0.1%, and the same DMSO concentrations were used in vehicle controls.

Cells

Lewis lung carcinoma cells (catalog # CRL-1642) were obtained from American Type Culture Collection (Manassas, VA) and maintained according to cell culture techniques suggested by the supplier.

Real-time Reverse Transcription–Polymerase Chain Reaction

Real-time reverse transcription–polymerase chain reaction (RT-PCR) analysis was performed as previously described [20]. Total RNA was isolated from cells using the RNeasy Mini kit (Qiagen, Valencia, CA). Real-time RT-PCR was carried out on ABI PRISM 7900HT Sequence Detection System (PE Applied Biosystems, Foster City, CA). Primer pairs and 6-carboxy-fluorescein–labeled probes for murine adenosine receptors and β-actin were provided by Applied Biosystems. Reverse transcription–polymerase chain reactions using 1 μg of DNase-treated total RNA were performed under conditions recommended by the manufacturer. A standard curve for each amplicon was obtained using serial dilutions of total RNA. The results from triplicate polymerase chain reactions for a given gene at each time point were used to determine mRNA quantity relative to the corresponding standard curve. The relative mRNA quantity for a given gene measured from a single reverse transcription reaction was divided by the value obtained for β-actin to correct for fluctuations in input RNA levels and varying efficiencies of reverse transcription reactions.

Measurement of cAMP Accumulation

Cyclic AMP accumulation was measured as previously described [21]. Lewis lung carcinoma cells were grown in 12-well plates to confluency. Cells were then preincubated in Tyrode's buffer (150 mM NaCl, 2.7 mM KCl, 0.37 mM NaH_2PO_4, 1 mM $MgSO_4$, 1 mM $CaCl_2$, 5 g/L D-glucose, 10 mM HEPES-NaOH, pH 7.4) containing 1 U/ml adenosine deaminase and the cAMP phosphodiesterase inhibitor papaverine (1 mM) for 10 minutes at 37°C. Adenosine receptor agonists, antagonists, or their vehicle (DMSO) were added to cells, and the incubation was allowed to proceed for 5 minutes at 37°C. The reaction was stopped by the addition of 1:5 volume of 25% trichloroacetic acid. The extracts were washed five times with 10 volumes of water-saturated ether. Cyclic AMP concentrations were determined using a cAMP assay kit (GE Healthcare, Little Chalfont, UK).

Mice

All studies were conducted in accordance with the Guide for the Care and Use of Laboratory Animals as adopted and promulgated by the US National Institutes of Health. Animal studies were reviewed and approved by the institutional animal care and use committee of Vanderbilt University. Seven- to eight-week-old age- and sex-matched mice were used. A_{2B}KO mice were obtained from Deltagen (San Mateo, CA), and wild type C57BL/6 mice were purchased from Harlan World Headquarters (Indianapolis, IN). Genotyping protocols for A_{2B}KO have been previously described [22]. All of the A_{2B}KO mice used in these studies were backcrossed to the C57BL/6 genetic background for 10 generations.

Isograft Tumor Model

Lewis lung carcinoma cells were dislodged from cell culture plates by repetitive pipetting with sterile PBS and then pelleted by centrifugation at 300*g* for 10 minutes. Cells were resuspended in PBS and counted using a hemocytometer. Final concentration was adjusted to

5×10^6 cells/ml, and 100 μl of cell suspension was injected subcutaneously into the right flank using a tuberculin syringe and a 27-gauge needle. Tumor volume was determined by external measurements using equation, $V = [L \times W^2] \times 0.5$, where V is volume, L is length, and W is width according to published methods [23]. Animals were inspected daily; the time was recorded and plotted as percentage of survival if mice were found dead or moribund and were euthanized at the discretion of the veterinarian blinded to animal group assignments. In all events, tumors did not exceed 2 cm in diameter or 10% of animal weight. To determine tumor weight, total cell number, and a proportion of tumor-infiltrating host immune cells, mice were killed at time points indicated under the Results section. To prepare single-cell suspensions, extracted tumors were chopped into small pieces, incubated in Dulbecco's modified Eagle's medium (DMEM) with 10% FBS, 1500 U/ml collagenase (Sigma), and 1000 U/ml hyaluronidase (Sigma) for 1 hour at 37°C, and then passed through a cell strainer. Total cell numbers were counted, and $CD45^+$ cell populations that represent tumor-infiltrating host immune cells were analyzed by flow cytometry.

Fluorescence-Activated Cell Sorting

After treatment with FcR Blocking Reagent (Miltenyi Biotec Inc., Auburn, CA), tumor single-cell suspensions (10^6 cells/ml) were labeled using fluorescein isothiocyanate (FITC)–conjugated anti-CD3e (clone 145-2C11), CD11c (clone HL3), Ly-6C/Gr-1 (clone RB6-8C5), phycoerythrin-conjugated anti-CD11b (clone M1/70), CD19 (clone 1D3), and peridinin-chlorophyll-protein–conjugated anti-CD45 (clone 30-F11) for 20 minutes on ice. All antibodies were obtained from BD Bioscience Pharmingen (San Jose, CA). Data acquisition was performed on a FACScalibur flow cytometer (BD Immunocytometry Systems, Franklin Lakes, NJ), and the data were analyzed with WinList 5.0 software. Nonviable cells were excluded by using 7-amino actinomycin D. Antigen negativity was defined as having the same fluorescent intensity as the isotype control.

Magnetic Cell Separation

Tumor-infiltrating host immune cells were magnetically separated from isograft tumor cells using CD45 magnetic microbeads following application protocols of the manufacturer (Miltenyi Biotec Inc.). In brief, after treatment with FcR Blocking Reagent, tumor single- cell suspensions (10^7 cells in 90 μl) were incubated with 10 μl of CD45 microbeads at 4°C for 15 minutes. The cells were then washed and resuspended in dilution buffer for magnetic cell separation. The labeled cells were passed through LS+ separation columns that had been equilibrated with dilution buffer. The CD45-negative cells were washed off the column three times with 3 ml of dilution buffer. The retained CD45-positive cells were eluted from the column outside the magnetic field by pipetting 5 ml of dilution buffer onto the column.

Analysis of Vascular Endothelial Growth Factor (VEGF) A Release and VEGF Protein Tissue Levels

To determine VEGF release from LLC cells in culture, cells were grown to confluency in 12-well plates. One hour before the experiment, the growth medium was replaced with DMEM containing 1× antibiotic-antimycotic mixture (Sigma) and 1 U/ml adenosine deaminase. Cells were incubated in the presence or absence of adenosine agonists and antagonists in the same medium for 6 hours under humidified atmosphere of air/CO_2 (19:1) at 37°C. To determine the effect of exogenously added adenosine on VEGF release, adenosine deaminase was excluded from the incubation medium in those particular experiments. Cell culture supernatants were collected for VEGF assay.

To compare VEGF protein levels in tumors extracted from WT and A_{2B}KO mice, tumor tissue (30 mg) was homogenized in 300 μl of RIPA lysis buffer using a pellet mixer (VWR Scientific, Marietta, GA). Tissue homogenates were incubated at 4°C for 30 minutes and then centrifuged at 16,000*g* for 20 minutes. Protein concentrations were measured using BCA Protein Assay Kit (Pierce, Rockford, IL). After adjusting protein concentrations to 1 mg/ml, supernatants were used to assay VEGF concentrations.

To determine VEGF release from tumor cell populations, magnetically separated $CD45^+$ and $CD45^-$ cells were counted and then pelleted by centrifugation. $CD45^+$ cells were resuspended at a concentration of 5×10^6 cells/ml in RPMI-1640 medium supplemented with 10% FBS, 1× antibiotic-antimycotic mixture, 1× nonessential amino acids (Sigma), 50 μM β-mercaptoethanol, and 1 U/ml adenosine deaminase. $CD45^-$ cells were resuspended at the same concentration in DMEM supplemented with 10% FBS, 1× antibiotic-antimycotic mixture, and 1 U/ml adenosine deaminase. Cells were incubated in the presence or absence of 10 μM NECA for 16 hours under humidified atmosphere of air/CO_2 (19:1) at 37°C. Vascular endothelial growth factor concentrations in supernatants were measured using an ELISA kit (R&D Systems, Minneapolis, MN).

Tumor Perfusion Assay

Fifteen minutes before euthanasia, mice received intravenous injections of FITC-labeled dextran (MWt 2,000,000; Sigma) for visualization of blood vessels. Tumors were extracted and fixed in 10% formalin; 7-μm sections were prepared across their middle part. Adjacent sections were either stained with hematoxylin-eosin or left unstained for fluorescence microscopy. Fluorescent images were taken from tumor sections, and the number of tumor blood vessels identified by dextran-FITC fluorescence was counted using a fluorescent microscope (Axiophot; Zeiss, Thornwood, NY). Only areas of viable tumor tissue were imaged; necrotic regions and overlying subdermal regions were excluded. For each section, four random images were captured under low magnification (objective, ×10) and analyzed by an investigator blinded to the origin of tumors. Vessels that were visibly interconnected were scored only once. The final vascular density score represents an average of all scored fields.

Statistical Analysis

Data were analyzed using the GraphPad Prism 4.0 software (GraphPad Software Inc., San Diego, CA) and presented as mean ± SEM. Comparisons between treatment groups and a control untreated group were performed using one-way ANOVA followed by Dunnett's posttests. Comparisons between two groups were performed using two-tailed unpaired *t* tests. Survival curves were compared using Mantel-Haenszel log rank test. A P value < .05 was considered significant.

Results

Lewis Lung Carcinoma Cells Express Functional Adenosine A_{2B} Receptors

Real-time RT-PCR showed that LLC cells preferentially express mRNA encoding A_{2B} receptors (0.204 ± 0.005% of β-actin; Figure 1*A*). Very low levels of A_{2A} receptor mRNA were also detected

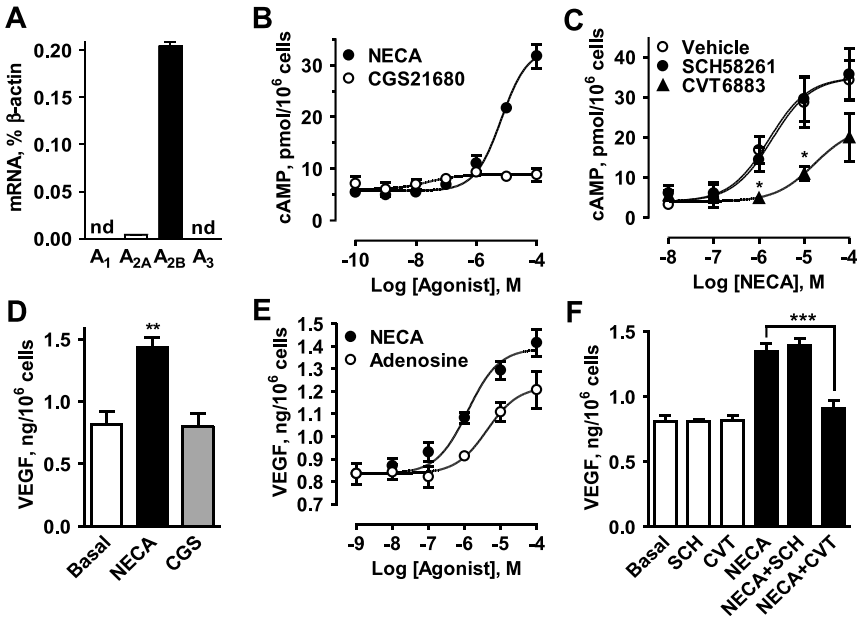

Figure 1. Characterization of adenosine receptors in LLC cell culture. (A) Real-time RT-PCR analysis of mRNA encoding adenosine receptor subtypes was performed as described under the Materials and Methods section. Values are expressed as mean of two determinations made in triplicate; *nd* indicates no transcripts detected. (B) Effects of the nonselective adenosine receptor agonist NECA and the A_{2A} adenosine receptor selective agonist CGS21680 on cAMP accumulation. Values are expressed as mean ± SEM, $n = 3$. (C) Effects of the selective A_{2A} antagonist SCH58261 (100 nM) and the selective A_{2B} antagonist CVT-6883 (100 nM) on NECA-induced cAMP accumulation. Values are expressed as mean ± SEM, $n = 3$. Asterisks indicate significant difference (*$P < .05$, unpaired two-tailed *t* tests) between NECA-induced cAMP accumulation in the presence of CVT-6883 and vehicle. (D) Effects of 10 μM NECA and 1 μM CGS21680 on VEGF release. Values are expressed as mean ± SEM, $n = 4$. Asterisks indicate significant difference (**$P < .01$, one-way ANOVA with Dunnett's posttest) compared to basal. (E) Effects of adenosine and its stable analog NECA on VEGF release. Values are expressed as mean ± SEM, $n = 3$. (F) Effects of 100 nM SCH58261 (SCH, SCH + NECA) and 100 nM CVT-6883 (CVT, CVT + NECA) or their vehicle (Basal, NECA) on VEGF release in the absence (Basal, SCH, CVT) or in the presence of 10 μM NECA (NECA, SCH + NECA, CVT + NECA). Values are expressed as mean ± SEM, $n = 3$. Asterisks indicate significant difference (***$P < .001$, one-way ANOVA with Bonferroni's posttest) between NECA-induced VEGF release in the presence of CVT-6883 and vehicle.

(0.004 ± 0.001% of β-actin), whereas transcripts for A_1 and A_3 receptors were below detection levels.

A_{2A} and A_{2B} receptors are known to stimulate adenylate cyclase through coupling to G_s proteins [5]. Therefore, we measured cAMP accumulation as a way to determine whether expression of mRNA translates into functional presence of adenosine receptors in LLC cells. As seen in Figure 1*B*, the nonselective adenosine receptor agonist NECA stimulated cAMP accumulation 5.9 ± 0.4-fold at a maximal concentration of 100 μM, whereas the selective A_{2A} agonist CGS21680 had no significant effect. Furthermore, the selective A_{2B} antagonist CVT-6883 [24], but not the selective A_{2A} antagonist SCH58261 [25,26], inhibited NECA-induced cAMP accumulation (Figure 1*C*).

Lewis lung carcinoma cells tonically release VEGF (Figure 1*D*). Stimulation of A_{2B} receptors with NECA, but not A_{2A} receptors with CGS21680, significantly increased VEGF release from 0.81 ± 0.1 to 1.44 ± 0.08 ng/10^6 cells ($P < .01$, $n = 4$, one-way ANOVA with Dunnett's posttest; Figure 1*D*). The nonselective agonists adenosine and its stable analog NECA both stimulated VEGF production in a concentration-dependent manner with estimated EC_{50} values of 4.2 and 1.2 μM, respectively (Figure 1*E*), close to their reported affinity at A_{2B} receptors [5,6]. In contrast, the selective A_{2A} agonist CGS21680 at a concentration 50 times exceeding its reported binding affinity (K_i) at A_{2A} receptors [5] had no effect on VEGF release from LLC cells (Figure 1*D*). Furthermore, only the selective A_{2B} antagonist CVT-6883, but not the selective A_{2A} antagonist SCH58261, inhibited NECA-stimulated VEGF secretion (Figure 1*F*). On the basis of these data, we concluded that that LLC cells express functional A_{2B} receptors linked to the up-regulation of VEGF release.

Prolonged Survival and Attenuated Tumor Growth in A_{2B}KO Mice

To test the hypothesis that host A_{2B} receptors could be exploited by tumors for their advantage, we examined whether tumor growth was suppressed in A_{2B}KO mice relative to WT control animals. The survival of A_{2B}KO mice was significantly prolonged compared with WT control animals after subcutaneous injection of LLC cells (Figure 2*A*). The tumor growth, expressed as either tumor volume (Figure 2*B*) or weight (Figure 2*C*), was significantly attenuated in A_{2B}KO compared to WT hosts. Of interest, an increase in tumor volume was retarded by 3 to 4 days in A_{2B}KO compared to WT hosts (Figure 2*B*), whereas a median survival value for A_{2B}KO mice was 5 days longer compared to WT control animals (Figure 2*A*). It is possible that the relationship between tumor size and survival is not linear; that is, a relatively small reduction in tumor size leads to a significant survival benefit. Alternatively, it is also possible that in addition to a reduced tumor size, other factors can also contribute to the prolonged survival of A_{2B}KO hosts. Taken together, our results suggest that the engaging of host A_{2B} adenosine receptors can be beneficial for tumors and detrimental for host survival.

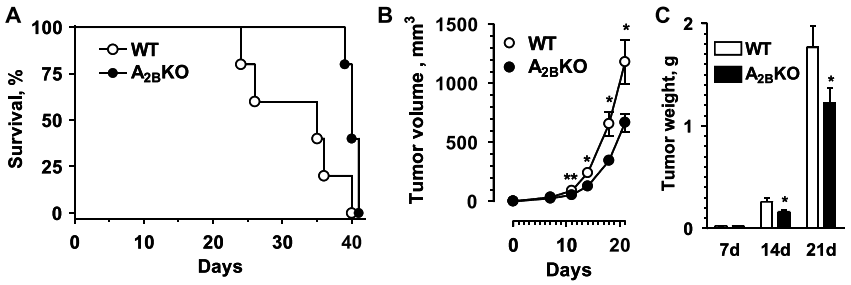

Figure 2. Increased host survival and decreased tumor size in mice lacking A_{2B} adenosine receptors. (A) Survival plot of WT and A_{2B}KO mice after subcutaneous injection of LLC cells in isograft tumor model as described under the Materials and Methods section. Mantel-Haenszel log rank test revealed significant difference in survival curves between WT and A_{2B}KO mice ($P = .02$, $n = 5$), with median survival values of 35 and 40 days for WT and A_{2B}KO mice, respectively. (B–C) Tumor growth of LLC was significantly attenuated in A_{2B}KO compared to WT mice. Tumor volume (B) was determined by direct measurement of tumor dimensions using calipers. Tumor weight (C) was determined by direct weighting of tumors extracted from euthanized animals on days 7 (7d), 14 (14d), and 21 (21d) after subcutaneous injection of LLC cells. Data are presented as mean ± SEM of five animals in each group. Asterisks indicate significant difference (*$P < .05$, **$P < .01$, unpaired two-tailed t tests) in corresponding values between WT and A_{2B}KO mice.

Flow Cytometry Analysis of Tumor-Infiltrating Host Immune Cells

Total cell numbers in single-cell suspensions obtained from tumors extracted from WT mice were higher than those in A_{2B}KO mice (Figure 3*A*), reflecting the attenuation of tumor growth in animals lacking A_{2B} receptors. However, flow cytometric analysis of tumor single-cell suspensions revealed that the proportion of tumor-infiltrating $CD45^+$ host immune cells (LLC cells are CD45-negative) was similar in tumors extracted from WT and A_{2B}KO mice on any given day after LLC inoculation. The percentage of $CD45^+$ cells in the total tumor cell population obtained from WT and A_{2B}KO mice was 14.4 ± 1.1% and 13.7 ± 1.9%, respectively, on day 7, increasing to 30.8 ± 1% and 28.8 ± 3.9% by day 14, and then slightly decreasing to 23.3 ± 3.1% and 22.8 ± 1.6% by day 21 (Figure 3*B*).

Because the percentage of $CD45^+$ cells was the highest 14 days after LLC inoculation, we chose this time point for further characterization of host tumor–infiltrating immune cell populations (Figure 4). $CD45^+$ cells were gated (Figure 4*A*) and analyzed for the expression of lymphoid lineage cell markers CD19 (B lymphocytes) and CD3e (T lymphocytes) and of myeloid lineage cell markers CD11b, CD11c, and Gr-1. We found that cells expressing markers of lymphoid lineage represented a minor population of tumor-infiltrating host immune cells (Figure 4*B*), whereas most cells expressed the common myeloid cell marker CD11b (Figure 4*C*). A considerable proportion of CD11b-positive cells expressed low levels of CD11c (Figure 4*C*). CD11b-positive cell population also included a subset of $CD11b^{high}/Gr\text{-}1^{high}$ cells (Figure 4*D*). The percentage of $CD11b^+/CD11c^-$ cells in tumor-infiltrating immune cells from WT and A_{2B}KO mice was 56.3 ± 1% and 46.4 ± 2.7%, respectively, whereas the percentage of $CD11b^+/CD11c^{low}$ cells was 42.3 ± 0.7% and 44 ± 1%, respectively. Greater (about threefold) differences between tumor-infiltrating immune cell populations in WT and A_{2B}KO mice were found for $CD3e^+$ cells (2.6 ± 0.3% and 8.7 ± 1.4%, respectively; $P < .001$, $n = 5$) and $CD11b^{high}/Gr\text{-}1^{high}$ cells (19.5 ± 1.4% and 6.7 ± 0.7%, respectively; $P < .001$, $n = 5$).

Host A_{2B} Adenosine Receptors Regulate VEGF Tumor Tissue Levels

Because A_{2B} receptors are known to regulate VEGF production in many cell types [10,16,21,27], we next examined the potential role of host A_{2B} receptors in regulating tumor VEGF levels. On day 14 after LLC inoculation, tissue VEGF protein levels were significantly lower in the tumors extracted from A_{2B}KO mice, compared to WT animals (75.7 ± 6.7 *vs* 126.3 ± 6.5 pg/mg, $P = .012$, $n = 3$; Figure 5*A*). It is possible that the lower intratumoral VEGF levels in A_{2B}KO mice may reflect the smaller size of the tumors, resulting in lower degrees of hypoxia and interstitial adenosine concentrations. It is also possible that A_{2B}KO host cells are phenotypically distinct, with reduced VEGF production in tumor tissues. To assess the latter possibility, we prepared single-cell suspensions from tumors extracted from WT and A_{2B}KO mice and magnetically separated $CD45^+$ cells from $CD45^-$ cells. As seen in Figure 5*B*, $CD45^+$ cells isolated from tumors grown in WT mice expressed mRNA encoding adenosine receptor subtypes with the rank order of transcript levels $A_{2B} > A_{2A} > A_3$, whereas $CD45^+$ cells isolated from tumors grown in A_{2B}KO mice exhibited similar levels of transcripts for A_{2A} and A_3 subtypes but lacked mRNA encoding A_{2B} receptors, reflecting the host origin of these cells. In contrast, expression levels of transcripts for A_{2B} receptors in $CD45^-$ cells isolated from tumors grown in WT and A_{2B}KO mice were virtually the same, indicating their common origin primarily from inoculated LLC cells expressing A_{2B} receptors (Figure 5*B*). Incubation of unstimulated tumor-infiltrating $CD45^+$ cells from a WT host for 16 hours resulted in accumulation of low levels of VEGF in cell culture medium (Figure 5*C*). Activation of adenosine receptors with 10 μM NECA in a fivefold increase in VEGF release from 22.7 ± 1.3 to 117.1 ± 5.1 pg/10^6 cells. Stimulation of VEGF secretion was dramatically reduced in tumor-infiltrating A_{2B}KO $CD45^+$ cells, indicating that secretion in tumor-infiltrating WT $CD45^+$ cells was mediated mainly through A_{2B} adenosine receptors. In contrast, tumor $CD45^-$ cells grown in WT and A_{2B}KO mice were characterized by similar basal and NECA-stimulated VEGF secretion (Figure 5*C*). Thus, our data indicate that the reduction in tumor tissue VEGF levels observed in A_{2B}KO mice could be accounted for by the loss of A_{2B} receptor–mediated regulation of VEGF secretion in tumor-infiltrating host immune cells. Consistent with reduced tumor tissue VEGF levels, we observed a lower density of FITC-dextran–perfused vessels in tumors grafted in A_{2B}KO mice when compared with tumors from WT mice (Figure 6).

Discussion

Due to their high metabolic activity and hypoxic environment, solid tumors are characterized by increased release of adenosine [28]. In this study, we used LLC cells that were previously demonstrated to release high levels of adenosine into the extracellular space under hypoxic conditions [4]. Extracellular adenosine levels within tumors have been shown to reach micromolar concentrations [3,4], suggesting that all adenosine receptor subtypes, including the low-affinity A_{2B} receptor, can be activated in this pathophysiological environment [6,29]. We have previously demonstrated in several different cell cultures that up-regulation of angiogenic factors is an important function of A_{2B} adenosine receptors [10,16,21,27]. Because A_{2B} receptors are expressed in various cancerous cells [8–14] and overexpressed in primary tumors [15,30], it is possible that these receptors could promote tumor angiogenesis by up-regulating VEGF levels. Indeed, our data show that cultured LLC cells preferentially express functional A_{2B} adenosine receptors and that their stimulation with the stable adenosine analog NECA results in up-regulation of VEGF secretion. These results correlate with our previous finding that stimulation of A_{2B} receptors in the human glioblastoma cell line U87MG up-regulates secretion of angiogenic factors [10], suggesting that A_{2B} receptors expressed on cancerous cells can promote tumor angiogenesis and hence their growth.

In addition to A_{2B} receptors located on cancerous cells, we now report that A_{2B} receptors in host tumor–infiltrating cells also up-regulate tumor VEGF levels. We found that LLC tumors grown in host animals lacking A_{2B} adenosine receptors contained significantly lower levels of VEGF and displayed lower intratumor vascular density compared to tumors grown in WT animals. This difference in neovascularization and tumor tissue VEGF levels was due to the A_{2B} receptor–dependent VEGF production by host tumor–associated cells, because stimulation of adenosine receptors in WT tumor-infiltrating $CD45^+$ immune cells with NECA produced a robust fivefold increase in VEGF production, an effect not seen in tumor-associated $CD45^+$ immune cells lacking A_{2B} adenosine receptors. In contrast, $CD45^-$ tumor cells were characterized by elevated tonic VEGF release, but NECA increased VEGF secretion only by 1.6-fold. Furthermore, we found no significant difference in VEGF production between $CD45^-$ tumor cells isolated from WT and A_{2B}KO mice. Thus, our data suggest that cancerous cells stimulate neovascularization not only by secreting VEGF on their own, but also by exploiting A_{2B} adenosine receptor–dependent regulation of VEGF production by host tumor–infiltrating immune cells to help promote tumor growth.

Indeed, assessment of several parameters of tumor growth in WT and A_{2B}KO mice supports this hypothesis. A_{2B}KO mice exhibited

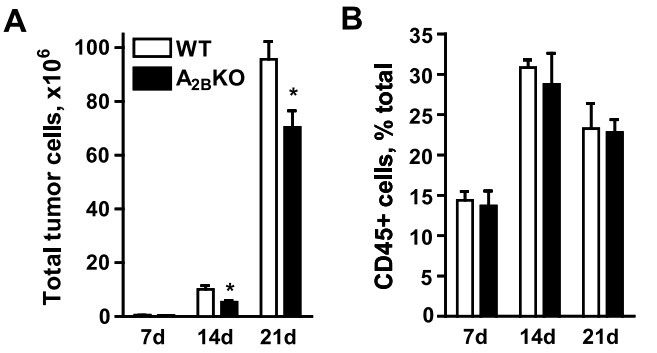

Figure 3. LLC tumors in WT and A_{2B}KO mice contain similar proportions of tumor-infiltrating host immune cells. Single-cell suspensions were obtained as described under the Materials and Methods section from LLC tumors extracted on days 7 (7d), 14 (14d), and 21 (21d) after subcutaneous injection of LLC cells in WT and A_{2B}KO mice. (A) Total cell numbers were counted using a hemocytometer. Total cell numbers in tumors extracted on day 7 from A_{2B}KO and WT mice were $0.40 \pm 0.06 \times 10^6$ and $0.47 \pm 0.04 \times 10^6$ cells, respectively. (B) Percentage of $CD45^+$ cells in total tumor cell population was determined by flow cytometry as described under the Materials and Methods section. Data are presented as mean ± SEM of three animals in each group. Asterisks indicate significant difference (*$P < .05$, unpaired two-tailed *t* tests) in corresponding values between WT and A_{2B}KO mice.

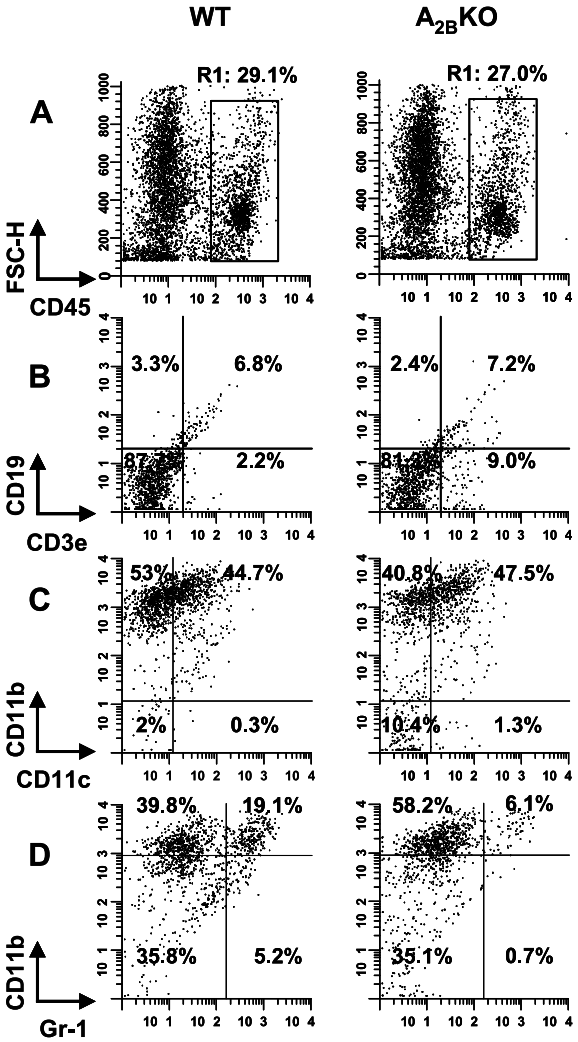

Figure 4. Expression of lymphoid and myeloid cell markers on the surface of tumor-infiltrating host immune cells. (A) Single-cell suspensions were prepared from tumors extracted from WT and A_{2B}KO mice on day 14 after inoculation with LLC cells. $CD45^+$ cells were gated for flow cytometry analysis of host immune cells infiltrated into tumor tissues. (B) Cytofluorographic dot plots of lymphoid cell marker CD19 and CD3e expression in $CD45^+$ cell populations. (C) Cytofluorographic dot plots of myeloid cell marker CD11b and CD11c expression in $CD45^+$ cell populations. (D) Cytofluorographic dot plots showing percentage of Gr-$1^{high}$$CD11b^{high}$ cells in $CD45^+$ cell populations. Representative data from flow cytometry analysis of cells obtained from six WT (left panels) and five A_{2B}KO animals (right panels) are shown.

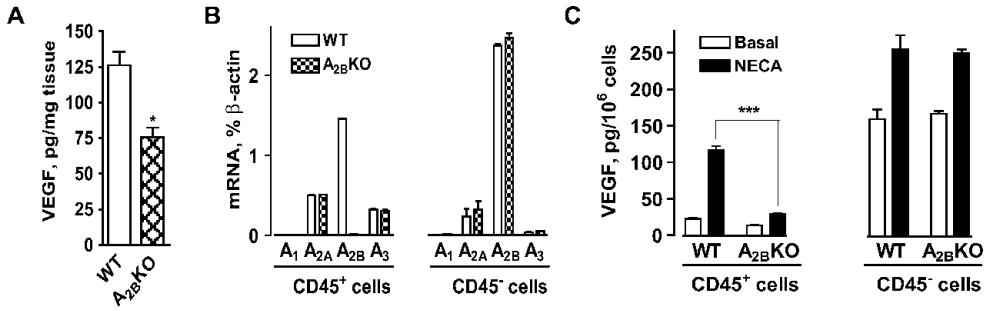

Figure 5. Host A_{2B} adenosine receptors regulate VEGF tumor tissue levels. (A) VEGF protein levels in tumors extracted from WT and A_{2B}KO mice on day 14 after inoculation with LLC cells. Data are presented as mean ± SEM of three animals in each group. Asterisk indicates significant difference (*$P < .05$, unpaired two-tailed t test) between WT and A_{2B}KO mice. (B) Real-time RT-PCR analysis of adenosine receptor subtype expression in $CD45^+$ and $CD45^-$ cells magnetically separated from single-cell suspensions obtained from tumors extracted from WT and A_{2B}KO mice on day 14 after inoculation with LLC cells as described under the Materials and Methods section. Results are presented as average of triplicate measurements after two independent cell separations. (C) Release of VEGF from tumor-infiltrating host $CD45^+$ cells and tumor $CD45^-$ cells was measured in conditioned medium after incubation of cells in the absence (Basal) or presence of 10 μM NECA for 16 hours. Data are presented as mean ± SEM of VEGF secretion from cells separately isolated from six animals in each group. Asterisks indicate significant difference (***$P < .001$, unpaired two-tailed t test) between WT and A_{2B}KO mice.

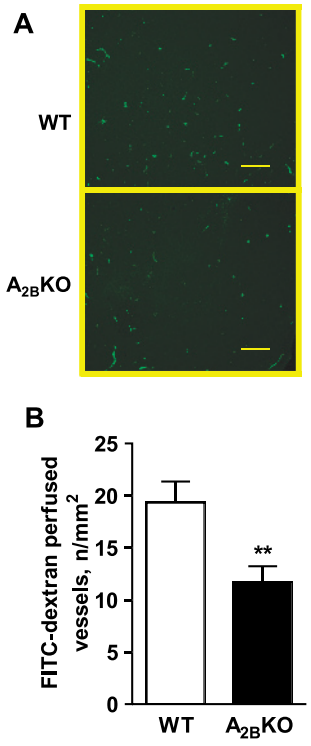

Figure 6. Decreased density of FITC-dextran perfused vessels in LLC tumors grown in A_{2B}KO mice. Intratumoral blood vessels were marked *in vivo* by FITC-dextran on day 14 after subcutaneous injection of LLC cells in WT and A_{2B}KO mice as described under the Materials and Methods section. (A) Representative fluorescence micrographs of blood vessels in LLC tumors grown in WT or A_{2B}KO mice. Scale bar, 200 μm. (B) Vessel counts obtained by morphometric analysis of LLC tumors. Data are expressed as number of FITC-dextran perfused vessels (n) per mm^2 of viable tumor tissue. Asterisks indicate significant difference (**$P < .01$, $n = 9$, unpaired two-tailed t test) between WT and A_{2B}KO mice.

significantly attenuated tumor growth and longer survival times compared with WT controls. Despite the significant difference in tumor size, weight, and total number of tumor cells, the dynamics of tumor infiltration with immune cells were similar in WT and A_{2B}KO mice as judged by the percentage of $CD45^+$ cells in total tumor cell populations. Two weeks after LLC inoculation, host $CD45^+$ cells represented about a third of total tumor cell populations in both WT and A_{2B}KO mice. Our data also show that the overwhelming majority of $CD45^+$ cells (~90%) also expressed a common myeloid cell marker CD11b indicating their myeloid lineage. Although tumor-associated myeloid cells have been previously suggested to be a significant source of VEGF [31], the novelty of our findings is that stimulation of A_{2B} adenosine receptors by tumor-produced adenosine plays an important role in VEGF secretion by these host tumor–infiltrating cells resulting in enhanced tumor neovascularization and growth.

Although the percentage of host cells infiltrating the tumor and the time course of this influx was similar between A_{2B}KO and WT mice, we found important differences in the subpopulations of $CD45^+$ cells. In particular, we found that the proportion of $CD11b^{high}/Gr\text{-}1^{high}$ cells was threefold lower in tumors grown in A_{2B}KO mice compared to WT control. In contrast, the proportion of cells expressing CD3e chains of T cell receptor was threefold higher in tumor-infiltrating $CD45^+$ cells isolated from A_{2B}KO mice compared to WT control. These findings may reflect differences in antitumor immune responses between A_{2B}KO and WT mice. Recent evidence suggests that immature myeloid cells accumulating in tumors play an important role in tumor escape from immune surveillance by suppressing T-cell responses. In mice, these myeloid cells are characterized as $CD11b^+/Gr\text{-}1^+$ cells [32] that decrease expression of CD3e chains of T-cell receptor in lymphocytes infiltrating the LLC tumors [33]. Our observations raise the interesting possibility that host A_{2B} receptors not only stimulate tumor angiogenesis but also suppress immune surveillance, thus engaging two distinct mechanisms to promote tumor survival and growth. These seemingly independent mechanisms could be related. We have previously

demonstrated that VEGF exerts multiple effects on immune cells and plays a critical role in the aberrant hemopoiesis [34–36]. Of interest, VEGF strongly inhibited T-cell development and increased the production of $CD11b^{high}/Gr\text{-}1^{high}$ myeloid cells in mice [34,36]. Therefore, it is possible that the difference in the expression of Gr-1 and CD3e markers in $CD45^+$ cells isolated from tumors grown in WT and A_{2B}KO cells is a reflection of different tumor tissue VEGF levels found in this study. However, we cannot exclude a direct immunosuppressive effect of A_{2B} receptors. It has been recently suggested that intratumoral adenosine protects cancerous tissues by inhibiting incoming antitumor T lymphocytes and natural killer cells through stimulation of A_{2A} and A_{2B} receptors [4,37]. This putative immunosuppressive role of A_{2B} receptors was inferred from studies in A_1, A_{2A}, and A_3 adenosine receptor knockout mice, but this hypothesis was not tested directly using A_{2B}KO mice. Assessment of a potential role of A_{2B} receptors in suppression of host immune surveillance would provide additional rationale for the development of A_{2B} antagonists as novel antitumor therapeutic adjunct agents.

It should be noted that our studies were designed to selectively determine the role of A_{2B} receptors in host cells. We also detected proangiogenic A_{2B} receptors in tumor cells, but we did not assess their contribution to adenosine-dependent stimulation of tumor growth. It is possible, therefore, that our tumor size and survival analysis underestimate the total importance A_{2B} receptor activation has on tumor growth. Targeting the low-affinity A_{2B} receptor, as opposed to other adenosine receptor subtypes, in the development of antitumor agents is especially appealing because this receptor is likely activated only in the pathophysiological tumor environment, while remaining silent in normal tissues [6]. This characteristic would provide specificity in targeting tumors, while decreasing the likelihood of side effects.

In summary, our study revealed for the first time that solid tumors characterized by an elevated adenosine release can exploit adenosine-dependent regulation of VEGF production by host tumor–associated immune cells. We found that host A_{2B} adenosine receptors up-regulate tumor tissue VEGF levels and increase intratumor vascular density in a mouse LLC isograft model, thus promoting tumor growth and decreasing host survival. Although our study focused primarily on A_{2B} receptor–mediated VEGF regulation, it is likely that other growth factors and complementary A_{2B} receptor–dependent mechanisms (e.g., immunosuppression) may also contribute to tumor growth.

Acknowledgments

The authors thank Luiz Belardinelli, Dewan Zeng, and Hongyan Zhong (CV Therapeutics, Inc., Palo Alto, CA) for scientific discussions related to these studies.

References

[1] Linden J (2006). Adenosine metabolism and cancer. Focus on "Adenosine downregulates DPPIV on HT-29 colon cancer cells by stimulating protein tyrosine phosphatases and reducing ERK1/2 activity via a novel pathway". *Am J Physiol* **291**, C405–C406.

[2] Lukashev D, Ohta A, and Sitkovsky M (2007). Hypoxia-dependent anti-inflammatory pathways in protection of cancerous tissues. *Cancer Metastasis Rev* **26**, 273–279.

[3] Blay J, White TD, and Hoskin DW (1997). The extracellular fluid of solid carcinomas contains immunosuppressive concentrations of adenosine. *Cancer Res* **57**, 2602–2605.

[4] Raskovalova T, Huang X, Sitkovsky M, Zacharia LC, Jackson EK, and Gorelik E (2005). G_s protein–coupled adenosine receptor signaling and lytic function of activated NK cells. *J Immunol* **175**, 4383–4391.

[5] Fredholm BB, Ijzerman AP, Jacobson KA, Klotz KN, and Linden J (2001). International Union of Pharmacology. XXV. Nomenclature and classification of adenosine receptors. *Pharmacol Rev* **53**, 527–552.

[6] Fredholm BB, Irenius E, Kull B, and Schulte G (2001). Comparison of the potency of adenosine as an agonist at human adenosine receptors expressed in Chinese hamster ovary cells. *Biochem Pharmacol* **61**, 443–448.

[7] Feoktistov I and Biaggioni I (1997). Adenosine A_{2B} receptors. *Pharmacol Rev* **49**, 381–402.

[8] Feoktistov I and Biaggioni I (1993). Characterization of adenosine receptors in human erythroleukemia cells. Further evidence for heterogeneity of adenosine A_2 receptors. *Mol Pharmacol* **43**, 909–914.

[9] Feoktistov I and Biaggioni I (1995). Adenosine A_{2B} receptors evoke interleukin-8 secretion in human mast cells. An enprofylline-sensitive mechanism with implications for asthma. *J Clin Invest* **96**, 1979–1986.

[10] Zeng D, Maa T, Wang U, Feoktistov I, Biaggioni I, and Belardinelli L (2003). Expression and function of A_{2B} adenosine receptors in the U87MG tumor cells. *Drug Dev Res* **58**, 405–411.

[11] Panjehpour M, Castro M, and Klotz KN (2005). Human breast cancer cell line MDA-MB-231 expresses endogenous A_{2B} adenosine receptors mediating a Ca^{2+} signal. *Br J Pharmacol* **145**, 211–218.

[12] Phelps PT, Anthes JC, and Correll CC (2006). Characterization of adenosine receptors in the human bladder carcinoma T24 cell line. *Eur J Pharmacol* **536**, 28–37.

[13] Rodrigues S, De Wever O, Bruyneel E, Rooney RJ, and Gespach C (2007). Opposing roles of netrin-1 and the dependence receptor DCC in cancer cell invasion, tumor growth and metastasis. *Oncogene* **26**, 5615–5625.

[14] Gessi S, Merighi S, Varani K, Cattabriga E, Benini A, Mirandola P, Leung E, Mac LS, Feo C, Baraldi S, et al. (2007). Adenosine receptors in colon carcinoma tissues and colon tumoral cell lines: focus on the A_3 adenosine subtype. *J Cell Physiol* **211**, 826–836.

[15] Li S, Huang S, and Peng SB (2005). Overexpression of G protein–coupled receptors in cancer cells: involvement in tumor progression. *Int J Oncol* **27**, 1329–1339.

[16] Feoktistov I, Ryzhov S, Goldstein AE, and Biaggioni I (2003). Mast cell–mediated stimulation of angiogenesis: cooperative interaction between A_{2B} and A_3 adenosine receptors. *Circ Res* **92**, 485–492.

[17] Merighi S, Benini A, Mirandola P, Gessi S, Varani K, Simioni C, Leung E, Maclennan S, Baraldi PG, and Borea PA (2007). Caffeine inhibits adenosine-induced accumulation of hypoxia-inducible factor-1alpha, vascular endothelial growth factor, and interleukin-8 expression in hypoxic human colon cancer cells. *Mol Pharmacol* **72**, 395–406.

[18] O'Byrne KJ and Dalgleish AG (2001). Chronic immune activation and inflammation as the cause of malignancy. *Br J Cancer* **85**, 473–483.

[19] Bingle L, Brown NJ, and Lewis CE (2002). The role of tumour-associated macrophages in tumour progression: implications for new anticancer therapies. *J Pathol* **196**, 254–265.

[20] Ryzhov S, McCaleb JL, Goldstein AE, Biaggioni I, and Feoktistov I (2007). Role of adenosine receptors in the regulation of angiogenic factors and neovascularization in hypoxia. *J Pharmacol Exp Ther* **382**, 565–572.

[21] Feoktistov I, Goldstein AE, Ryzhov S, Zeng D, Belardinelli L, Voyno-Yasenetskaya T, and Biaggioni I (2002). Differential expression of adenosine receptors in human endothelial cells: role of A_{2B} receptors in angiogenic factor regulation. *Circ Res* **90**, 531–538.

[22] Scoka B, Nemeth ZH, Virag L, Gergely P, Leibovich SJ, Pacher P, Sun C-X, Blackburn MR, Vizi ES, Deitch EA, et al. (2007). A_{2A} adenosine receptors and C/EBPbeta are crucially required for IL-10 production by macrophages exposed to *E. coli*. *Blood* **110**, 2685–2695.

[23] Williams CS, Tsujii M, Reese J, Dey SK, and DuBois RN (2000). Host cyclooxygenase-2 modulates carcinoma growth. *J Clin Invest* **105**, 1589–1594.

[24] Sun CX, Zhong H, Mohsenin A, Morschl E, Chunn JL, Molina JG, Belardinelli L, Zeng D, and Blackburn MR (2006). Role of A_{2B} adenosine receptor signaling in adenosine-dependent pulmonary inflammation and injury. *J Clin Invest* **116**, 2173–2182.

[25] Zocchi C, Ongini E, Conti A, Monopoli A, Negretti A, Baraldi PG, and Dionisotti S (1996). The non-xanthine heterocyclic compound SCH 58261 is a new potent and selective A_{2A} adenosine receptor antagonist. *J Pharmacol Exp Ther* **276**, 398–404.

[26] Feoktistov I and Biaggioni I (1998). Pharmacological characterization of adenosine A_{2B} receptors: studies in human mast cells co-expressing A_{2A} an A_{2B} adenosine receptor subtypes. *Biochem Pharmacol* **55**, 627–633.

[27] Grant MB, Tarnuzzer RW, Caballero S, Ozeck MJ, Davis MI, Spoerri PE, Feoktistov I, Biaggioni I, Shryock JC, and Belardinelli L (1999). Adenosine receptor activation induces vascular endothelial growth factor in human retinal endothelial cells. *Circ Res* **85**, 699–706.

[28] Spychala J (2000). Tumor-promoting functions of adenosine. *Pharmacol Ther* **87**, 161–173.

[29] Merighi S, Mirandola P, Varani K, Gessi S, Leung E, Baraldi PG, Tabrizi MA, and Borea PA (2003). A glance at adenosine receptors: novel target for antitumor therapy. *Pharmacol Ther* **100**, 31–48.

[30] Xiang H, Liu Z, Wanga D, Chena Y, Yanga Y, and Dou K (2006). Adenosine A_{2b} receptor is highly expressed in human hepatocellular carcinoma. *Hepatol Res* **36**, 56–60.

[31] Dirkx AE, Oude Egbrink MG, Wagstaff J, and Griffioen AW (2006). Monocyte/macrophage infiltration in tumors: modulators of angiogenesis. *J Leukoc Biol* **80**, 1183–1196.

[32] Kusmartsev S and Gabrilovich DI (2006). Role of immature myeloid cells in mechanisms of immune evasion in cancer. *Cancer Immunol Immunother* **55**, 237–245.

[33] Rodriguez PC, Quiceno DG, Zabaleta J, Ortiz B, Zea AH, Piazuelo MB, Delgado A, Correa P, Brayer J, Sotomayor EM, et al. (2004). Arginase I production in the tumor microenvironment by mature myeloid cells inhibits T-cell receptor expression and antigen-specific T-cell responses. *Cancer Res* **64**, 5839–5849.

[34] Gabrilovich D, Ishida T, Oyama T, Ran S, Kravtsov V, Nadaf S, and Carbone DP (1998). Vascular endothelial growth factor inhibits the development of dendritic cells and dramatically affects the differentiation of multiple hematopoietic lineages *in vivo*. *Blood* **92**, 4150–4166.

[35] Dikov MM, Ohm JE, Ray N, Tchekneva EE, Burlison J, Moghanaki D, Nadaf S, and Carbone DP (2005). Differential roles of vascular endothelial growth factor receptors 1 and 2 in dendritic cell differentiation. *J Immunol* **174**, 215–222.

[36] Huang Y, Chen X, Dikov MM, Novitskiy SV, Mosse CA, Yang L, and Carbone DP (2007). Distinct roles of VEGFR-1 and VEGFR-2 in the aberrant hematopoiesis associated with elevated levels of VEGF. *Blood* **110**, 624–631.

[37] Ohta A, Gorelik E, Prasad SJ, Ronchese F, Lukashev D, Wong MK, Huang X, Caldwell S, Liu K, Smith P, et al. (2006). A_{2A} adenosine receptor protects tumors from antitumor T cells. *Proc Natl Acad Sci USA* **103**, 13132–13137.